

RSC Advances



This is an *Accepted Manuscript*, which has been through the Royal Society of Chemistry peer review process and has been accepted for publication.

Accepted Manuscripts are published online shortly after acceptance, before technical editing, formatting and proof reading. Using this free service, authors can make their results available to the community, in citable form, before we publish the edited article. This *Accepted Manuscript* will be replaced by the edited, formatted and paginated article as soon as this is available.

You can find more information about *Accepted Manuscripts* in the [Information for Authors](#).

Please note that technical editing may introduce minor changes to the text and/or graphics, which may alter content. The journal's standard [Terms & Conditions](#) and the [Ethical guidelines](#) still apply. In no event shall the Royal Society of Chemistry be held responsible for any errors or omissions in this *Accepted Manuscript* or any consequences arising from the use of any information it contains.

Cite this: DOI: 10.1039/c0xx00000x

www.rsc.org/xxxxxx

ARTICLE TYPE

Adsorption of rare earth metals (Sr²⁺ and La³⁺) from aqueous solution by Mg-aminoclay-humic acid [MgAC-HA] complexes in batch mode

Young-Chul Lee,^a Arunkumar Rengaraj,^b Taegong Ryu,^c Hyun Uk Lee,^d Ha-Rim An,^d Kug-Seung Lee,^e Go-Woon Lee,^f Jun Yeong Kim,^b Jungho Ryu,^c Byoung-Gyu Kim^{*c} and Yun Suk Huh^{*b}

Received (in XXX, XXX) Xth XXXXXXXXXX 20XX, Accepted Xth XXXXXXXXXX 20XX

DOI: 10.1039/b000000x

The recoveries of Sr²⁺ and La³⁺ as rare earth metals (REMs) were studied using Mg-aminoclay-humic acid [MgAC-HA] complexes prepared by self-assembled precipitation due to electrostatic attraction between water-solubilized [MgAC] and water-soluble [HA], and were compared with the recoveries using [MgAC] and [HA]. The influences of pH and Sr²⁺ and La³⁺ concentrations in single and binary systems were evaluated. The adsorbents before/after adsorption of Sr²⁺ and La³⁺ were characterized on (1) scanning electron microscopy (SEM) micrographs, (2) Fourier transform infrared (FT-IR), X-ray photoelectron spectroscopy (XPS), and extended X-ray absorption fine structure (EXAFS) spectra, and by (3) powder X-ray diffraction (XRD) pattern analysis. After fitting Langmuir and Freundlich isotherms, the Langmuir model was found to present better matches than the Freundlich one: the maximum adsorption capacities of Sr²⁺ and La³⁺ were 0.12 mg/g and 4.76 mg/g in the binary system at room temperature, and the optimal recovery pH was ~8.0. In practical seawater meanwhile, the recoveries of Sr²⁺ and La³⁺ by [MgAC-HA] complexes were the highest in the binary system. However, with further recycling runs, the recoveries of Sr²⁺ and La³⁺ were critically diminished due to disassembly in [MgAC-HA] complexes at acidic condition. Thus, for the purposes of industrial application, we are currently pursuing the enhancement of recyclability for [MgAC-HA] complexes by its encapsulation or direct hydrogel formation.

Introduction

Self-assembled precipitates (objects) of cationic nanoparticles and anionic macro-size polymers and vice versa have induced heterogeneous materials with unique properties,¹ resulting in matrixes of multifunctional groups. Particularly in energy and environmental sectors, electrostatic-interaction-based water-solubilized materials are highly attractive owing to their easy recovery and simple protocol.² Lee *et al.*, for example, reported that water-solubilized cationic Fe-aminoclay (FeAC) with graphene oxide in aqueous solution produced a precipitate showing that (nano)composites of Fe-aminoclay nanoparticles (FeAC NPs) uniformly decorated graphene oxide and, consequently, played as a heterogeneous Fenton-like system.³

Recently, cationic organo-building blocks of Mg-aminoclay [MgAC], as positively charged nanoclusters of 30 nm – 150 nm hydrodynamic diameter,⁴ induced water-soluble humic acid [HA] flocculation and were utilized in the harvesting of negatively charged microalgal cells.² Mg-aminoclay-induced humic acid [MgAC-HA] complexes have been easily produced by simple mixing, resulting in a network-like and precipitated matrix.² Furthermore, [MgAC] was established for mass production by simple sol-gel processing at room temperature⁵ with little or no ecotoxicity⁶ or cytotoxicity.⁷ On the other hand, [HA] with a high molecular weight distribution is known to function as a fraction in ubiquitous organic matter under environmentally relevant conditions.⁸ [HA] is insoluble at < pH 2.0 but soluble at neutral and basic pH. Particularly, [HA] has many functional groups such as phenolic OH, enolic OH, hydroxyl OH, methoxyls, quinones, aldehydes, ketones, and even thiols, which play a role in the reduction or capping of the sites of NPs.⁹

Taking into consideration the protonated and rich amine groups of [MgAC] and the negatively charged carboxylic and hydroxyl groups of [HA], [MgAC-HA] complexes can be a green adsorbent for cationic ion recovery with negligible inhibition by organic matter. In other words, such ion-exchange and chelating adsorption has been widely employed in the adsorption process for practical collection of radionuclides, precious metals, and ionic nutrients from aqueous solutions,¹⁰ traditionally.

Research in rare earth metals (REMs) and trace metals (TMs) such as lithium (Li), strontium (Sr), yttrium (Y), cerium (Ce), europium (Eu), and lanthanum (La) is booming due to shortages and depletion of reserves.¹¹⁻¹⁷ Indeed, their use in batteries, medical applications, surgical lasers, scintillation detectors, and other areas is expanding very rapidly.^{12-14,18,19} Recent research has been driven by the desire to find a relatively effective and economical means of REMs recovery in aqueous solution. Beyond extraction or recovery methods such as precipitation, ion exchange, filtration, solvent extraction and others, adsorption techniques including biosorption are among the simple and economically feasible choices.^{10-14,17,20-23} [MgAC-HA] complexes were tested for recyclability, and overall REMs recovery efficiency (%), and feasibility in seawater media against only-[MgAC] and [HA]. Representative Sr²⁺ and La³⁺ as single and binary systems were the targeted. In order to reveal the interactive mechanism between adsorbents and REMs, the microscopic investigations of Sr²⁺ and La³⁺ in [MgAC-HA] complexes by X-ray photoelectron spectroscopy (XPS) and extended X-ray absorption fine structure (EXAFS) methods were tested.²⁴⁻²⁶

Materials and methods

Materials and methods. Humic acid sodium salt (denoted [HA]), 3-aminopropyltriethoxysilane (denoted APTES, $\geq 98\%$, 221.37 g/mol), magnesium chloride hexahydrate ($\text{MgCl}_2 \cdot 6\text{H}_2\text{O}$), strontium nitrate ($\text{Sr}(\text{NO}_3)_2$, 211.63 g/mol), La (III) nitrate ($\text{La}(\text{NO}_3)_3 \cdot 6\text{H}_2\text{O}$, 433.01 g/mol), phenolphthalein, Na_2CO_3 , and NaHCO_3 were purchased from Sigma-Aldrich (MO, USA). Bulk ethanol solvent (18L, 95%) was obtained from Samchun Pure Chemicals (Gyeonggi-do, Korea) for preparation of Mg-aminoclay [MgAC]. The 1L standard 0.1/1.0 M HCl and NaOH solutions were acquired from Samchun company (Gyeonggi-do, Korea). Double-distilled deionized water (denoted DI water; resistance: 18 $\text{M}\Omega \cdot \text{cm}$ at 25°C) was employed for preparation of all of the samples.

Preparation of Mg-aminoclay [MgAC]. The [MgAC] preparation procedure followed the literature.²⁷ Briefly, 8.4 g of $\text{MgCl}_2 \cdot 6\text{H}_2\text{O}$ was added to 200 mL of ethanol solution and subjected to 10 min magnetic stirring resulting in fully dissolved homogeneous solution. Then, to this solution, 13 mL of APTES was added, adjusting the molar ratio of Mg:Si to approximately 1.33. Immediately, white-colored slurry was produced. By 5 min centrifugation at 6000 \times g, and after washing once with 500 mL of bulk ethanol solution and subsequent oven drying, the precipitate was finally prepared as white [MgAC] powder using a mortar and pestle.

[HA] precipitation by [MgAC] ([MgAC-HA] complexes). Based on the Lee *et al.* research to be reported,² it was different results in the previous reports. In this study, [HA] with water-solubilized and negatively charged properties was intended to utilize precipitation by water-solubilized and cationic [MgAC] in aqueous solution. [HA] stock solution of 0.2 g/L concentration and [MgAC] solution (5 g/L) were separately prepared. 15 mL of [HA] stock solution and 5 mL of [MgAC] solution were mixed, according to the optimal condition for higher precipitates. After 5 min centrifugation at 6000 \times g, the supernatant was removed. The remaining precipitates were washed with 10 mL of DI water. After repeated centrifugation at 6000 \times g for 5 min, the remaining precipitate in an insoluble form (~ 5 mg/mL) was utilized for adsorbent of REMs (Sr^{2+} and La^{3+}).

Batch adsorption tests. 100 mg/L Sr^{2+} and La^{3+} stock solutions were prepared by dissolving 0.2624 mg/L strontium (II) nitrate and 0.2338 mg/L lanthanum (III) nitrate in DI water, respectively. The adsorbent property of the [MgAC-HA] complexes was determined in both single (Sr^{2+} or La^{3+}) and binary (Sr^{2+} and La^{3+}) mixture solutions. In glass vials containing 9 mL of the 55.6 mg/L stock Sr^{2+} and/or La^{3+} solutions, 1 mL containing 5 mg of the [MgAC], [HA], and as-prepared [MgAC-HA] complexes, respectively, was added, thus forming ~ 50 mg/L Sr^{2+} and La^{3+} ions. These sample solutions were pH-adjusted with 0.1/1.0 M HCl and NaOH standard solutions. After 8 hrs equilibrium, at certain sampling points the supernatants of the centrifuged Sr^{2+} and La^{3+} solutions were analyzed by inductively coupled plasma optical emission spectrometry (ICP-OES; Varian 720-ES, USA). Parameters such as pH (3-11) and adsorbent dosage for stock solutions were tested ranging from 50 to 500 mg/L. The efficiencies (%) of Sr^{2+} and La^{3+} recovery from the aqueous

solution were calculated by the equation

$$\text{Recovery efficiency (r, \%)} = \frac{C_0 - C_t}{C_0} \times 100 \quad (1)$$

The effective recovery (adsorption) efficiency (%) was calculated by subtraction of the Sr^{2+} and La^{3+} precipitation ratio (%) according to the pH.

The amounts (%) of Sr^{2+} and La^{3+} from the aqueous solution were calculated by the equation

$$q_e = \frac{V}{m} \quad (2)$$

The amounts of Sr^{2+} and La^{3+} adsorbed (mg/g) q_e were determined by the equation (2),

where C_0 is the initial concentration of Sr^{2+} and La^{3+} , C_t is the concentration (mg/L) of Sr^{2+} and La^{3+} at time t , V is the volume of adsorbate (L), and m is the weight of the adsorbent (g). Based on adsorption capacity and mechanism studies, Langmuir (monolayer adsorption) and Freundlich (heterogeneous surface and multilayer adsorption) models were formulated.²⁸ The Langmuir equation is

$$\frac{C_e}{q_e} = \frac{1}{K_L q_m} + \frac{C_e}{q_m} \quad (3),$$

where C_e (mg/L) is the equilibrium concentration of Sr^{2+} or La^{3+} , q_e is the amount of adsorbed Sr^{2+} or La^{3+} at equilibrium (mg/g), q_m is the maximum adsorption capacity, and K_L is the Langmuir constant relative to the adsorption capacity. In contrast, the Freundlich equation is

$$\ln q_e = \ln K_F + \frac{1}{n} \ln C_e \quad (4),$$

where n is the Freundlich exponent (i.e., heterogeneity coefficient) and K_F is the Freundlich constant relative to the adsorbent affinity. After plotting of the Langmuir and Freundlich equations, the K_L/q_m and K_F/n were summarized respectively.

Recovery and recycling tests in seawater media. Real seawater was collected at Incheon port near Ulmi-do, Korea (approximate N latitude: 37.4594575, E longitude: 126.6256454). For the Sr^{2+} and La^{3+} recycling runs, the initial concentrations selected were 250, 100, and 50 mg/L. For the adsorbents ([MgAC], [HA], and [MgAC-HA] complexes), the experimental procedures outlined in “[HA] precipitation by [MgAC] ([MgAC-HA] complexes)” were followed. With the seawater, 5 mL of [MgAC-HA] complexes or 5 mL containing 25 mg of [MgAC] and [HA] or 45 mL of Sr^{2+} and La^{3+} solution was mixed for 8 hrs. After 5 min centrifugation at 6000 \times g, the separated [MgAC-HA] complexes were treated with 1.0 N HNO_3 to recover the Sr^{2+} and La^{3+} salts. Then, it was utilized for more two cycles. All of the graphs were plotted with averaged values from three replicates.

Characterizations of adsorbents ([MgAC], [HA], and [MgAC-HA] complexes). Morphological micrographs of the adsorbents were examined under HITACHI S-4300 scanning electron microscopy (SEM) equipped with an energy-dispersive X-ray (EDX) detector. Powder X-ray diffraction (XRD, RIGAKU, D_{MAX} 2500) patterns were recorded using Cu K α radiation between 3° and 80° at a rate of 2 θ /degree. Small-angle X-ray diffractometer (SAXS, RIGAKU, D/MAX-2500) spectra with 18 kW generator were recorded at 2 θ =0.3-2.0° as transmission mode. Fourier transform infrared (FT-IR) spectroscopy using KBr pellets in the transmission mode between 400 and 4,000 cm^{-1} was performed using a Bruker VERTEX 80V spectrometer to determine the organic vibration bondings. Zeta potential of [MgAC] in aqueous solution was measured by Zetasizer Nano-ZS particle analyzer (Malvern, UK). The pH values were monitored using a Thermo Scientific pH meter (Thermo Scientific™ Orion™, MA, USA).

In order to microscopic Sr_{3d} and La_{3d} interaction of oxygen (O) and nitrogen (N) species in [MgAC-HA] complexes with Sr^{2+} and

La³⁺ ions by recording of X-ray photoelectron spectroscopy (XPS) with monochromatic Al K α X-ray radiation ($h\nu = 1486.6$ eV) operated at 120W (Kratos Analytical, AXIS Nova, Manchester, UK).²⁹

Furthermore, the O interaction in [MgAC-HA] complexes with Sr²⁺ and La³⁺ by extended X-ray absorption fine structure (EXAFS).³⁰ In detail, X-ray absorption fine structure (XAFS) was measured at 8C nano-probe XAFS beamline (BL8C) of Pohang Light Source (PLS-II) in the 3.0 GeV storage ring, with a ring current of 320 mA. The radiation source of BL8C is a tapered in-vacuum-undulator. The X-ray beam was monochromated by a Si (111) double crystal and then it was delivered to a secondary source aperture where the beam size was adjusted to be 0.3 mm (v) \times 1 mm (h). A high voltage (3000 V) was applied to ionization chambers which were filled with N₂/Ar mixture gases to detect x-ray intensity. XAFS measurement was conducted in a transmission mode. The obtained spectra were processed using Demeter software. EXAFS spectra were fitted in a Fourier-transform range of 2 – 10 \AA^{-1} for Sr K-edge and 2 – 9 \AA^{-1} for La L₃-edge data. All fitting was conducted with a Hanning window between 1 \AA and 3.5 \AA . To fit the EXAFS spectra Sr(OH)₂ and La(OH)₃ model paths were used. The amplitude reduction factor (S_0^2) was set to be 1.0 during the fitting both Sr and La absorption data.

For the measurement of acidic surface functional groups in [HA] and [MgAC-HA] complexes, it was followed.³¹ Briefly, 0.2 g of each samples was added in difference base solutions (0.1 M NaOH, 0.1 M Na₂CO₃, and 0.05 M NaHCO₃) and mixed overnight at room temperature. After preparation of 10 mL of sample solution, 15 mL of 0.1 M HCl was added and titrated again with 0.1 M NaOH to endpoints with phenolphthalein indicator. The NaOH-titrable acidities were considered as total acidic surface functional groups but NaHCO₃-titrable acidities were considered to carboxyl groups. The differences between NaOH-titrable acidities and Na₂CO₃-titrable acidities/NaHCO₃-titrable acidities and Na₂CO₃-titrable acidities were associated with phenol and lactone groups, respectively.

Results and discussion

Characteristics of [HA] sedimentation using [MgAC] ([MgAC-HA] complexes)

Schematically, as shown in Figure 1, [MgAC]-decorated macromolecular [HA] induced precipitates of net-work-like matrixes.² Water-solubilized clay clusters with positively charged zeta-potential interacted with water-soluble [HA] macromolecules with negatively charged surfaces. For zeta potential of [MgAC] at 1.0 g/L at pHs (2.0-12.0) (Supplementary Information Figure S1), it showed positively charged surface ($> +20$ mV) in a wide pH region but slightly lower cationic property, corresponding to the literature.^{32,33} SEM images of the pristine [MgAC] and [HA] along with the [MgAC-HA] complexes dispersed in DI water are displayed in Supplementary Information, Figure S2. [MgAC] showed a smooth surface with some rugged and granulated aspects. However, [HA] showed a distinct plate-like morphology, suggestive of pillars of morphological shape. Significantly, as shown in Figure 2, [MgAC-HA] complexes, by [MgAC] coating onto the [HA] surface, exhibited a more rugged and uneven surface than that of

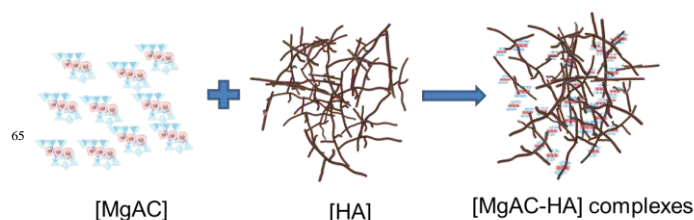


Fig. 1 Schematic representation of self-assembled [MgAC-HA] complexes with [HA] and [MgAC]. The [MgAC] and [HA] possess positively and negatively charged surfaces, respectively.

pristine [MgAC]. After Sr²⁺ or La³⁺ and the mixture of Sr²⁺ and La³⁺ in the [MgAC-HA] complexes, the SEM microphotographs presented rougher and more porous structures by ionic binding or metal hydroxide forms of REM salts, indicating that the REMs salts had been adsorbed on them, similarly to the previous morphology of the [MgAC-HA] complexes. Also, this was confirmed with the Sr- and La-elemental compositions by EDX analysis (Fig. 2g). In order to examine the crystallinity and impurities in the adsorbents ([MgAC], [HA], and [MgAC-HA] complexes), the powder XRD patterns were investigated (Fig. 3a). Generally, [MgAC] revealed a typical magnesium phyllosilicate with 2:1 smectite clay, confirmed at $d_{060,330}=0.16$ nm ($2\theta=59$) and corresponding to the reported aminoclays by Mann *et al.*³⁴ In detail, at $d_{001}=1.80$ nm, with the sharp reflection peak, $d_{020,110}=0.40$ nm, $d_{130,200}=0.26$ nm in the higher angles was matched with [MgAC]. By contrast, [HA] showed the typical iron silicon carbide (JCPDS 018-0651), graphite (JCPDS 026-1079), and chaoite (JCPDS 022-1069). Even in the [MgAC-HA] complexes, both [MgAC] and [HA] peaks were observed, indicating that organic-vibrations existed in both. The distinct basal spacing at d_{001} was shifted to a low angle. When [MgAC]

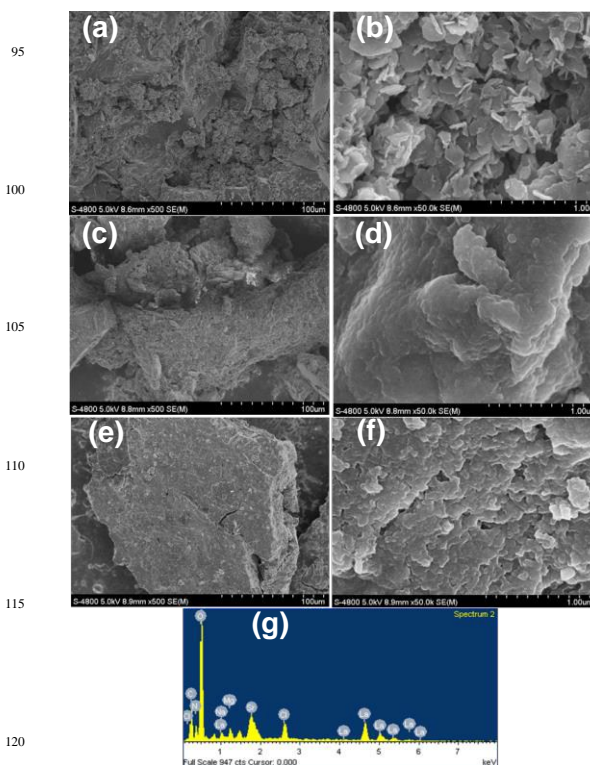


Fig. 2 Scanning electron microscopy (SEM) images of (a,b) Sr²⁺, (c,d) La³⁺ and (e,f) mixture of Sr²⁺ and La³⁺ adsorbed by [MgAC-HA] complexes and (g) elemental compositions in [MgAC-HA] complexes by 125 energy-dispersive X-ray (EDX) analysis.

underwent the re-assembly process with [HA]. In small angle X-ray scattering (SAXS) data at lower angle (Supplementary Information, Figure S3) in [MgAC], [HA], [MgAC-HA] complexes, and mixture of Sr^{2+} and La^{3+} adsorbed [MgAC-HA] complexes resulted in $d=200.55 \text{ \AA}$ at $2\theta=0.440$, none, $d=290.23 \text{ \AA}$ at $2\theta=0.304$, and $d=294.18 \text{ \AA}$ at $2\theta=0.304$, respectively. It is indicated that [HA] molecules were intercalated into organo-building blocks of [MgAC] and subsequently re-assembled precipitate, i.e., [MgAC-HA] complexes. In other words, [HA] was intercalated into the clay layers. As a result, the mesolamellar distance at d-spacing in the [MgAC-HA] complexes was markedly increased.² Additionally, REMs could be intercalated into layers of [MgAC-HA] complexes. It is evident that d-spacing was increased $\sim 4 \text{ \AA}$ unit. Taking into consideration of 1.32 \AA and 1.06 \AA of Sr^{2+} and La^{3+} ionic radius, these REMs could be intercalated into [MgAC-HA] complexes. In order to investigate the organic functional groups and interaction sites in the adsorbents with Sr^{2+} and La^{2+} , the FT-IR spectra were analyzed (Fig. 3b). The vibration peaks matching of [MgAC] was recorded at $-\text{OH}/\text{Mg}-\text{OH}$ stretching vibration ($3,390 \text{ cm}^{-1}$), $-\text{CH}_2$ symmetric/asymmetric stretching vibrations ($2,956$ and 2884 cm^{-1}), $-\text{NH}_3^+$ stretching vibration ($2,020 \text{ cm}^{-1}$), $-\text{NH}_2$ bending vibration ($1,607 \text{ cm}^{-1}$), $-\text{CH}_2$ bending vibration ($1,501 \text{ cm}^{-1}$), C-N stretching vibration ($1,219 \text{ cm}^{-1}$), Si-C stretching vibration ($1,112 \text{ cm}^{-1}$), Si-O-Si stretching vibration ($1,017 \text{ cm}^{-1}$), $-\text{OH}$ deformation vibration of inner Mg-OH groups (933 cm^{-1}), N-H wagging vibration (746 cm^{-1}), and Mg-O stretching vibration (533 cm^{-1}), which corresponded to the pendent-functional groups of $-\text{NH}_2(\text{CH}_2)_3-$ and covalent bonding in inorganic brucite ($\text{Mg}(\text{OH})_2$) sheets in [MgAC],³⁵ indicating successful synthesis. For the spectra of the [HA] peaks, it exhibited specifically in the $3,345 - 3,223 \text{ cm}^{-1}$ regions of the N-H/ $-\text{OH}$ stretching vibration modes of alcohols/phenols, amines/amides, and carboxylic acid in this region.⁹ Although there was overlapped with the aromatic C-H vibration peaks, it was assigned at $2,926$ and $2,850 \text{ cm}^{-1}$ of C-H stretching vibration, at $1,558 \text{ cm}^{-1}$ of C=O and $1,378 \text{ cm}^{-1}$ in the carboxylate group and at $1,378 \text{ cm}^{-1}$ of CH_3/CH_2 bending vibrations. At $1,000 - 1,200 \text{ cm}^{-1}$, the stretching vibration of the C-O stretching vibration modes in the alcohols/phenols/ethers of the functional groups, and at $< 600 \text{ cm}^{-1}$ in the impurities of metal oxides, also were assigned. These spectral peaks in [HA] were in line with the reported literature.^{2,9} FT-IR spectra in [MgAC-HA] complexes showed distinct and weak peaks at CH_2 stretching vibration ($2,922 \text{ cm}^{-1}$), C=O stretching vibration at $1,554 \text{ cm}^{-1}$, CH_3/CH_2 bending vibrations at $1,378 \text{ cm}^{-1}$, C-O stretching vibration at $1,207 \text{ cm}^{-1}$, C-N stretching vibration at $1,207 \text{ cm}^{-1}$, Si-O-Si/C-O stretching vibrations at 998 cm^{-1} , and Mg-O stretching vibration

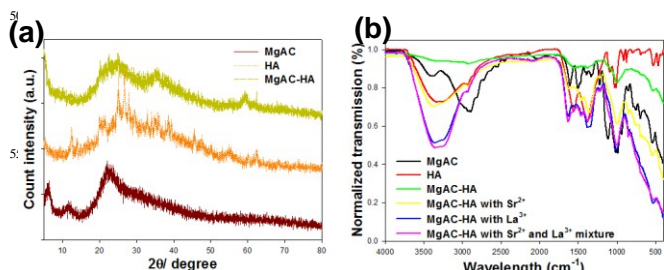


Fig. 3 (a) Powder X-ray diffraction (XRD) patterns of [MgAC], [HA], and [MgAC-HA] complexes and (b) Fourier transform infrared (FT-IR) spectra of [MgAC], [HA], [MgAC-HA] complexes, [MgAC-HA] complexes with Sr^{2+} , [MgAC-HA] complexes with La^{3+} , and [MgAC-HA] complexes with Sr^{2+} and La^{3+} mixture.

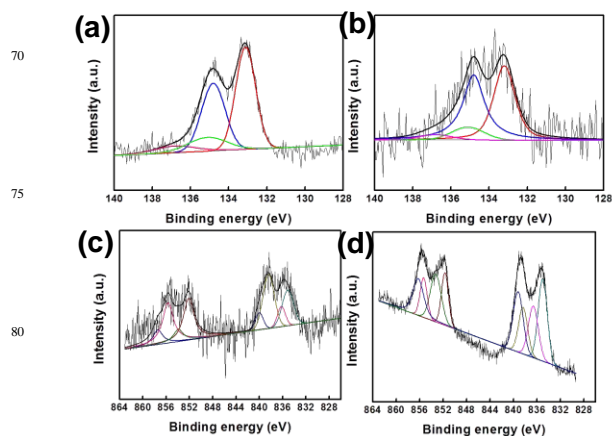


Fig. 4 Sr 3d binding energy (eV) of [MgAC-HA] complexes with Sr^{2+} (a) and with Sr^{2+} and La^{3+} mixture (b), and La 3d binding energy (eV) of [MgAC-HA] complexes with La^{3+} (c) and (b) with Sr^{2+} and La^{3+} mixture (d).

at 536 cm^{-1} . Particularly, the N-H/ $-\text{OH}$ stretching vibrations weakened and the $-\text{NH}_3^+$ stretching vibration disappeared, indicating that the N-H/ $-\text{OH}$ in the functional groups had strong interacting sites. Additionally, the Si-O-Si/ C-O stretching vibrations at 998 cm^{-1} were blue-shifted by about $\Delta 2-25 \text{ cm}^{-1}$. The carboxylic acids/alcohols/phenols/ethers of the functional groups revealed interaction sites for the self-assembled [MgAC-HA] complexes. In the cases of [MgAC-HA] complexes interaction with Sr^{2+} and La^{3+} , importantly, N-H/ $-\text{OH}$ in the functional groups was re-recorded at $3,348 - 3,245 \text{ cm}^{-1}$, and $-\text{CH}_2$ symmetric/asymmetric and $-\text{NH}_3^+$ stretching vibrations also re-appeared at $2,956/2,926 \text{ cm}^{-1}$ and at $2,084 \text{ cm}^{-1}$. The C=O stretching vibrations at $1,619-1,630 \text{ cm}^{-1}$ were observed at $\Delta 15-26 \text{ cm}^{-1}$, and the NH_2 bending vibrations at $1,459 \text{ cm}^{-1}$ as well as the CH_3/CH_2 bending vibration at $1,340 - 1,376 \text{ cm}^{-1}$ were red-shifted. The Si-C stretching vibration peak disappeared. Both C-O stretching vibration at $1,020 \text{ cm}^{-1}$ and Mg-O stretching vibration at 533 cm^{-1} were assigned without any peak shifts. As a result, the C=O groups in the carboxylic groups along with the $-\text{NH}_2$ groups in the primary amine groups of the [MgAC-HA] complexes indicated interactions of REMs rather than protonated amine ($-\text{NH}_3^+$) groups at neutral pH.^{27,36} Due to pH buffering effect of [MgAC-HA] complexes, the neutral pH was moderately maintained at about neutral pH after adding [MgAC-HA] complexes in Sr^{2+} and La^{3+} solution (Supplementary Information, Figure S4). Thus, the recovery mechanisms of Sr^{2+} and La^{3+} were considered to be complexation, ion exchange, and electrostatic interactions.¹¹ It was related to La^{3+} removal by magnetic alginate in the previous study.¹² However, magnetic alginate was related by exchange of La^{3+} ions.

The contents of acidic functional groups in [HA] and [MgAC-HA] complexes by titration method were measured, resulting in $2.54/8.8 \text{ mmol/g}$ and $1.1/4.4 \text{ mmol/g}$ of phenolic and lactone groups in [HA] and [MgAC-HA] complexes (Supplementary Information, Table S1). Although the total acidic surface functional groups in [MgAC-HA] complexes were decreased, primary amine groups of [MgAC] was added. Resultantly, diverse functional groups including both acidic and amine groups showed synergistically enhanced adsorption efficiency of REMs.

In order to reveal the interaction mechanism of oxygen (O) in [MgAC-HA] complexes with Sr^{2+} and La^{3+} , XPS spectra of O_{1s} and N_{1s} were recorded (Fig. 4). As shown in Supplementary

Information, Figure S5a, the survey scans of O_{1s}, N_{1s}, and C_{1s} in [MgAC-HA] complexes were detected. After interaction of Sr²⁺ or La³⁺ ions, it was detected in Sr²⁺, La³⁺, and Sr²⁺ and La³⁺

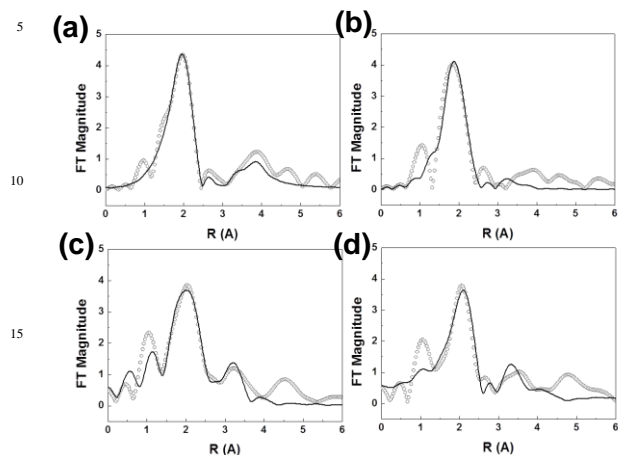


Fig. 5 Fourier-transformed EXAFS spectra and their fitting results of (a) [MgAC-HA] complexes with Sr²⁺, (b) [MgAC-HA] complexes with Sr²⁺ and La³⁺ mixture (Sr K-edge), (c) [MgAC-HA] complexes with La³⁺, (d) [MgAC-HA] complexes with Sr²⁺ and La³⁺ mixture (La L₃-edge).

mixture adsorbed onto [MgAC-HA] complexes (Supplementary Information, Figure S5b-d). Figure 4a displayed deconvolution fitting of Sr_{3d} binding energy with O [134.8/136.8 eV] and N [133.1/135.1 eV], O [134.8/136.8 eV] and N [133.2/135.1 eV] in Sr²⁺ (Fig. 4a) and mixture of Sr²⁺ and La³⁺ ions (Fig. 4b) adsorbed onto [MgAC-HA] complexes.³⁷ In contrast, that of La_{3d} binding energy with O [836.2/853.9 eV] and N [835.1/852.1 eV], O [836.5/853.2 eV] and N [834.9/851.6 eV] in La³⁺ (Fig. 4c) and mixture of Sr²⁺ and La³⁺ ions (Fig. 4d) adsorbed onto [MgAC-HA] complexes.^{38,39} Specific binding energy position, full width at half maximum (FWHM), and area in deconvolution curves was summarized (Supplementary Information, Table S2-5, respectively).

The results of EXAFS fitting are displayed (Fig 5 and Supplementary Information, Table S6). The fittings for Sr²⁺ and La³⁺ samples correspond well with their respective model paths while the fittings of both Sr K-edge and La L₃-edge for Sr²⁺ and La³⁺ samples do not correspond very well as observed in Figure 5 and the R-factor in Table S5. This indicates that the former two samples have structures similar to their model compounds. In the sample with Sr²⁺ and La³⁺ mixture, however, the structure is distorted by the introduction of the other metal. In addition, the uncertainty of the position and distances of the surrounding atoms is higher for metal-metal bondings than for the corresponding metal-O bondings as easily expected.

Adsorption of Sr²⁺ and La³⁺ in single and binary systems by adsorbents ([MgAC], [HA], and [MgAC-HA] complexes) according to pHs.

As preliminary adsorption experiments, within the initial 2 hrs reaction, most of the Sr²⁺ and La³⁺ REMs were adsorbed, and were saturated at < 12 hrs stirring (data not shown). According to the pHs (2, 4, 6, 8, 10, and 12), the recovery efficiencies (%) of Sr²⁺, La³⁺ and Sr²⁺/La³⁺ by [MgAC], [HA], and [MgAC-HA]

complexes in the single and binary systems are plotted in Figures 6-8, respectively. Taking into consideration Sr(OH)₂ and La(OH)₃ precipitation as related to the pH values, the recovery efficiencies (%) were calculated.²⁰ In the case of Figure 6a, [MgAC] in the single system showed 35.94% of Sr²⁺ and 28.54% of La³⁺ at pH 8.0 as well as 16.79% of Sr²⁺, and 32.97% of La³⁺ at pH 10.0. In the contrasting binary system, Figure 6b showed 15.58% of Sr²⁺ and 46.87% of La³⁺ at pH 8.0 as well as 37.6% of Sr²⁺ and 52.43% of La³⁺ at pH 10.0. Interestingly, the recoveries of Sr²⁺ and La³⁺ ions in the binary system were moderately enhanced, which meant that [MgAC] was not inhibited by the mixed ions. The optimal recovery pH of Sr²⁺ and La³⁺ recovery had been expected to fall within the pH ~8.0 - 10.0 range; the actual Sr²⁺ and La³⁺ ion removals by [HA] in the single (Fig. 7a) and binary (Fig. 7b) systems were as follows: 21.94% of Sr²⁺ and 16.54% of La³⁺ at pH 8.0 as well as 29.79% of Sr²⁺, and 16.97% of La³⁺ at pH 10.0 in the single system; 6.94% of Sr²⁺ and 21.22% of La³⁺ at pH 8.0 as well as 6.79% of Sr²⁺ and 25.02% of La³⁺ at pH 10.0 in the binary system. In general, the Sr²⁺ and La³⁺ recovery efficiencies (%) by [HA] were lower than those of [MgAC]. It was found that the primary amine functional groups in [MgAC] have better Sr²⁺ and La³⁺ recovery efficiencies (%) than the carboxyl acids/alcohols/phenols/ethers of the functional groups in [HA].¹⁷ Interestingly, the [MgAC-HA] complexes showed, as plotted in Figure 8, synergistic Sr²⁺ and La³⁺ recovery efficiencies (%) in the single and binary systems: specifically, 40.97% of Sr²⁺ and 39.15% of La³⁺ at pH 8.0 as well as 6.06% of Sr²⁺, and 56.29% of La³⁺ at pH 10.0 in the single system, and 40.97% of Sr²⁺ and 42.87% of La³⁺ at pH 8.0 as well as 6.06% of Sr²⁺ and 49.18% of La³⁺ at pH 10.0 in the binary system. The [MgAC-HA] complexes possessed better recovery efficiencies (%) than those of [MgAC] and [HA]. Indeed, the [MgAC-HA] complexes showed enhanced recoveries for both the Sr²⁺ and La³⁺ ions. At pH 10.0, there was significant recovery efficiency of La³⁺ ion, 56.29 and 49.18% in the single and binary systems respectively, but very low recovery efficiency of Sr²⁺ ion: 6.06 and 6.08% in the single and binary systems, respectively. However, at pH 8, even though the La³⁺ recovery efficiency was moderately reduced in both systems (single and binary), both the Sr²⁺ and La³⁺ recovery efficiencies were higher: 40.97/39.15% and 40.97/42.87% in the single and binary systems, respectively. From the viewpoint of the REM recovery by the [MgAC-HA] complexes in the binary system, for practical applications, the

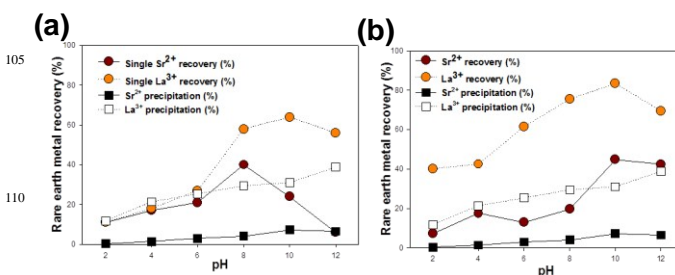


Fig. 6 Rare earth metal (REMs) recovery (%) of (a) single Sr²⁺ and La³⁺ and (b) mixture of Sr²⁺ and La³⁺ by [MgAC] according to pHs.

optimal pH was expected to be ~pH 8.0. In this pH region, it is significant that there are fewer protonated amine groups in [MgAC] and carboxylic/phenolic groups in [HA], and fewer precipitated REMs ions as well. Under these conditions, neutral amine groups and negatively charged [HA] macromolecules freely electrostatically interact with positively charged Sr²⁺ and La³⁺ ions.

Additionally to the recovery efficiencies, the adsorption isotherms under the equilibrium condition were studied with Langmuir (mostly monolayer adsorption) and Freundlich (major multiple adsorption sites) modeling (Supporting Information Figures S6-9). The parameter results from the two models are summarized in Table 1. In the cases of the [MgAC], [HA], and [MgAC-HA] complexes, most of the adsorbents were fitted better with the Langmuir equation than with the Freundlich one, the complexes can be employed as adsorbents of Sr²⁺ and La³⁺ in either the binary or more mixed system.

Table 1. Parameter results for Langmuir and Freundlich equilibrium models

Adsorbent	Langmuir			Freundlich		
	K _L	q _{max}	R ²	K _F	n	R ²
[MgAC] for Sr ²⁺ adsorption (single)	48.076	0.142	0.9636	0.327	5.73	0.919
[MgAC] for La ³⁺ adsorption (single)	23.809	1.54	0.9932	0.5945	2.02	0.9367
[MgAC] for Sr ²⁺ adsorption (binary)	21.123	0.056	0.982	0.352	1.07	0.921
[MgAC] for La ³⁺ adsorption (binary)	38.24	1.124	0.978	0.671	4.86	0.937
[HA] for Sr ²⁺ adsorption (single)	18.27	0.09	0.932	0.375	4.82	0.8684
[HA] for La ³⁺ adsorption (single)	51.68	0.172	0.988	0.375	4.82	0.8684
[HA] for Sr ²⁺ adsorption (binary)	43.47	0.017	0.954	0.213	3.16	0.925
[HA] for La ³⁺ adsorption (binary)	16.6	0.029	0.9824	0.62	2.31	0.925
[MgAC-HA] complexes for Sr ²⁺ adsorption (single)	0.020	0.029	0.978	0.0311	6.39	0.9389
[MgAC-HA] complexes for La ³⁺ adsorption (single)	2.38	5.050	0.996	0.150	8.628	0.9225
[MgAC-HA] complexes for Sr ²⁺ adsorption (binary)	10.82	0.12	0.921	3.53	2.690	0.852
[MgAC-HA] complexes for La ³⁺ adsorption (binary)	26.3	4.76	0.957	1.52	1.23	0.917

adsorption process of which is a predominant monolayer adsorption behavior based on an R² value of close to 1. The maximum adsorption capacities of [MgAC] for Sr²⁺ and La³⁺ in the single and binary systems were 0.142/1.54 and .0056/1.124 mg/g, respectively, indicating a lower maximum recovery capacity in the binary system than in the single system. Contrastingly, despite the relatively low recovery efficiencies in the case of [MgAC], the maximum adsorption capacities of HA for Sr²⁺ and La³⁺ in the single and binary systems were 0.090/0.172 and 0.017/0.029 mg/g, respectively. For n value > 1 in Freundlich model, it is matched with homogeneous sorption rather than heterogeneous one (Table 1). As for the [MgAC-HA] complexes, the maximum recovery capacities were 0.029/5.5050 and 0.120/4.760 mg/g in the single and binary systems, respectively. These results strongly suggest that [MgAC-HA] complexes can be employed as adsorbents of Sr²⁺ and La³⁺ in either the binary or more mixed system.

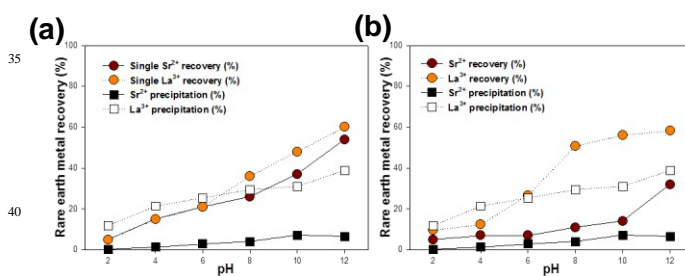


Fig. 7 REMs recovery (%) of (a) single Sr²⁺ and La³⁺ and (b) mixture of Sr²⁺ and La³⁺ by [HA] according to pHs.

Recovery of Sr²⁺ and La³⁺ in binary system by adsorbents ([MgAC], [HA], and [MgAC-HA] complexes) in seawater media at ~pH 8.0.

In order to study the feasibility of the concentrated 100 mg/L Sr²⁺ and La³⁺ mixture in real seawater without pH control, the Sr²⁺ and La³⁺ recovery efficiencies (%) in [MgAC], [HA], and the [MgAC-HA] complexes were 24.102/45.92%, 20.658/32.7%, and 37.192/74.68%, respectively, as plotted in Figure 9. In spite of in ionic media, the recovery patterns of Sr²⁺ and La³⁺ were similar. Still, the [MgAC-HA] complexes possessed synergistic recovery efficiencies (%). As a result, in the presence of other ions, the [MgAC-HA] complexes could successfully recover REMs at pH 8.0 in which the adsorption portion of REMs is highest than that of surface precipitates of REMs hydroxides. Interestingly, [MgAC] was enhanced to a pH value between 8.0 and 10.0 by protonated primary amine groups (Supporting Information, Figure S4) However, the [MgAC-HA] complexes were neutralized, and so the original seawater pH was adjusted ~8.0.

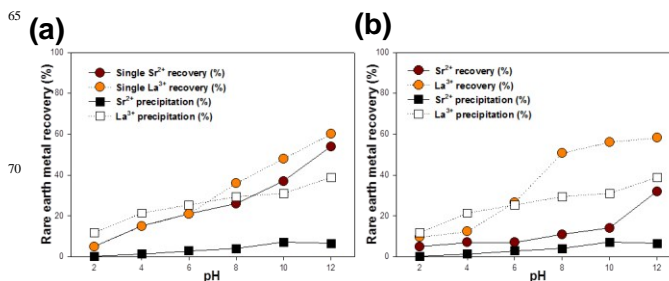


Fig. 8 REMs recovery (%) of (a) single Sr²⁺ and La³⁺ and (b) mixture of Sr²⁺ and La³⁺ by [MgAC-HA] complexes according to pHs.

Recycling runs of adsorbents ([MgAC], [HA], and [MgAC-HA]) for recovery of Sr²⁺ and La³⁺ mixtures in seawater media.

For evaluation of the economic feasibility of the adsorbents, Sr²⁺ and La³⁺ ion recycling tests of [MgAC], [HA], and the [MgAC-HA] complexes were performed at initial 250, 100, and 50 mg/L concentrations at pH ~8.0 in seawater media (Fig. 10). The recovery efficiencies (%) of Sr²⁺ at 250, 100, and 50 mg/L were ~82.14/88.86/88.04%, 4.75/6.09/7.66, and 2.8/7.83/16.59% in the first, second, and third runs respectively, while those of La²⁺ at 250, 100, and 50 mg/L were ~96.10/90.97/90.89%, 32.34/76.66/87.70, and 0.56/4.56/12.06% in first, second, and third runs. The recovery of the recyclability of Sr²⁺ was significantly lower than that of La³⁺ due to the latter's higher electrostatic attraction. When washing with adsorbents by 1.0N HNO₃,²² significant amounts of water-solubilized [MgAC] and [HA] were lost. [MgAC-HA] complexes also were lost in the de-assembly process. Because of disassembly in [MgAC-HA] complexes at acidic condition, so we are developing an alternative system of hydrogel formation by its encapsulation of [MgAC-HA] complexes or direct hydrogel formation of [MgAC] with sodium alginate. It is an emergent task for optimization process in recycling [MgAC-HA] complexes.

In the presence of 10 mg/L of [HA], adsorption of Sr²⁺ and La³⁺ ions onto [MgAC-HA] complexes was little affected because of working pH 7.0-8.0 (data not shown). It is agreement with Sheng *et al.*,^{40,41} in which at low pH values due to metal-bridging and ligand-bridging formation, humic substances promoted Ni²⁺ and Eu³⁺ interactions but at > pH 8.0 and inner-sphere surface complexes and surface precipitates were occurred.

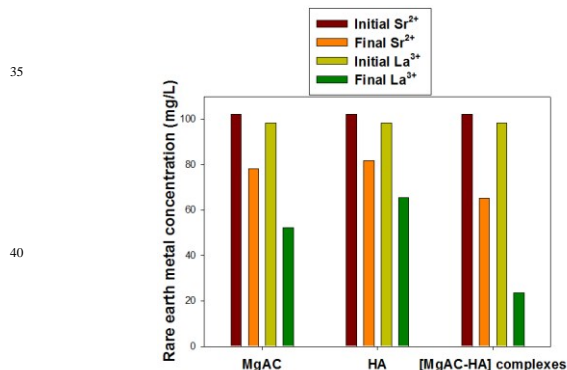


Fig. 9 REMs recovery (%) of Sr²⁺ and La³⁺ mixture at 100 mg/L in real seawater by [MgAC], [HA], and [MgAC-HA] complexes.

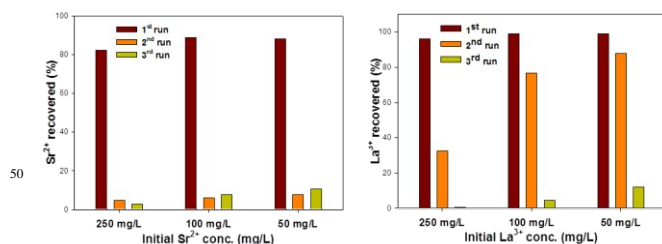


Fig. 10 Recycling tests of single (a) Sr²⁺ and (b) La³⁺ recovery (%) in real seawater by [MgAC-HA] complexes.

Conclusions

We designed biocompatible and non-toxic [MgAC-HA] complexes by self-assembled precipitation due to electrostatic interaction between protonated amine clusters in water-solubilized [MgAC] and water-soluble [HA] with negatively charged surfaces, i.e., [HA] macromolecules intercalation into layered [MgAC]. Those diverse, functionally enriched [MgAC-HA] complexes synergistically recovered Sr²⁺ and La³⁺ ions from seawater media, showing 0.12 and 4.76 mg/g adsorption capacities, following the Langmuir model. The optimal recovery pH was ~pH 8.0, which is similar in seawater. Although recycling runs for [MgAC-HA] complexes should find optimal extracting agents and conditions, with encapsulation or direct hydrogel formation could easily be controlled for practical application. So, taking into consideration the synergistic REMs recovery effect in [MgAC-HA] complexes, this effective, simple, and green adsorption technology helps us to further reduce the overall costs of REMs recovery.

Acknowledgements

This research was supported by a Gachon University research grant (GCU-2014-0125) as well as This work was supported by the General Research Project of the Korea Institute of Geoscience and Mineral Resources funded by the Ministry of Trade, Industry and Energy of Korea.

Notes and references

- ^aDepartment of BioNano Technology, Gachon University, 1342 Seongnamdaero, Sujeong-gu, Seongnam-si, Gyeonggi-do 461-701, Republic of Korea.
- ^bDepartment of Biological Engineering, College of Engineering, Inha University, Incheon 402-751, Republic of Korea.
- ^cMineral Resources Research Division, Korea Institute of Geoscience and Mineral Resources (KIGAM), Daejeon 305-350, Republic of Korea.
- ^dAdvanced Nano-Surface Research Group, Korea Basic Science Institute (KBSI), Daejeon 305-806, Republic of Korea.
- ^ePohang Accelerator Laboratory (PAL), Pohang 790-784, Republic of Korea
- ^fQuality Management Team, Korea Institute of Energy Research (KIER), 152 Gajeongro, Yuseong-gu, Daejeon 305-343, Republic of Korea.
E-mail: kgbkim@kigam.re.kr (Dr. B.-G.Kim)
E-mail: yunsuk.huh@inha.ac.kr (Prof. Y.S.Huh)
- 1 S. Mann, *Nat. Mater.*, 2009, **8**, 781-792.
- 2 Y.-C. Lee, S. Y. Oh, H. U. Lee, B. Kim, S. Y. Lee, M.-H. Choi, G.-W. Lee, J.-Y. Park, Y.-K. Oh, T. Ryu, Y.-K. Han, K.-S. Chung and Y. S. Huh, *Bioresour. Technol.*, 2014, **153**, 365-369.
- 3 Y.-C. Lee, S.-J. Chang, M.-H. Choi, T.-J. Jeon, T. Ryu and Y. S. Huh, *Appl. Catal. B-Environ.* 2013, **142-143**, 494-503.
- 4 A. J. Patil and S Mann, *J. Mater. Chem.*, 2008, **18**, 4605-4615.
- 5 Y.-C. Lee, E.S. Jin, S. W. Jung, Y.-M. Kim, K. S. Chang, J.-W. Yang, S.-W. Kim, Y.-O. Kim and H.-J. Shin, *Sci. Rep.*, 2013, **3**, 1292(1-8).
- 6 M.-H. Choi, Y. Hwang, H. U. Lee, B. Kim, G.-W. Lee, Y.-K. Oh, H. R. Andersen, Y.-C. Lee and Y. S. Huh, *Ecotox. Environ. Safe.*, 2014, **102**, 34-41.
- 7 H.-K. Han, Y.-C. Lee, M.-Y. Lee, A. J. Patil and H.-J. Shin, *ACS Appl. Mater. Interfaces*, 2011, **3**, 2564-2572.
- 8 B. Pan, B. S. Xing, W. X. Liu, S. Tao, X. M. Lin, X. M. Zhang, Y. X. Zhang, Y. Xiao, H. C. Dai and H. S. Yuan, *Environ. Pollut.*, 2006, **143**, 24-33.
- 9 N. Akaighe, R. I. MacCusprie, D. A. Navarro, D. S. Aga, S. Banerjee, M. Sohn and V. K. Sharma, *Environ. Sci. Technol.*, 2011, **45**, 3895-3901.
- 10 N. Das and D. Da, *J. Rare Earths*, 2013, **31**, 933-943.

- 11 D. Wu, J. Zhao, L. Zhang, Q. Wu and Y. Yang, *Hydrometallurgy*, 2010, **101**, 76-83.
- 12 D. Wu, L. Zhang, L. Wang, B. Zhu and L. Fan, *J. Chem. Technol. Biotechnol.*, 2011, **86**, 345-352.
- 13 F. Wang, J. Zhao, X. Wei, F. Huo, W. Li, Q. Hu and H. Liu, *J. Chem. Technol. Biotechnol.* 2014, **89**, 969-977.
- 14 H. Yang, W. Wang, H. Cui, D. Zhang, Y. Liu and J. Chen, *J. Chem. Technol. Biotechnol.*, 2012, **87**, 198-205.
- 15 F. Yang, F. Kubota, Y. Baba, N. Kamiya and M. Goto, *J. Hazard. Mater.*, 2013, **254-255**, 79-88.
- 16 Q. Tan, J. Li and X. Zeng, *Crit. Rev. Environ. Sci. Technol.*, 2015, **45**, 749-776.
- 17 D. Das, J. S. Varshini and N. Das, *Miner. Eng.*, 2014, **69**, 40-56.
- 18 M. S. Gasser and M. I. Aly, *Int. J. Miner. Process.*, 2013, **121**, 31-38.
- 19 X. Yang, J. Zhang and X. Fang, *J. Hazard. Mater.*, 2014, **279**, 384-388.
- 20 D. Song, S.-J. Park, H. W. Kang, S. B. Park and J.-I. Han, *J. Chem. Eng. Data*, 2013, **58**, 2455-2464.
- 21 H. M. Marwani, H. M. Albishri, T. A. Jalal and E. M. Soliman, *Arab. J. Chem.* 2013, <http://dx.doi.org/10.1016/j.arabjc.2013.01.008>.
- 22 C. Kütahyalı, Ş. Sert, B. Çetinkaya, S. Inan and M. Eral, *Sep. Sci. Technol.* 2010, **45**, 1456-1462.
- 23 M. H. Khani, *Sep. Sci. Technol.* 2012, **47**, 1886-1897.
- 24 G. Sheng, S. Yang, J. Sheng, J., Hu, X. Tan and X. Wang, *Environ. Sci. Technol.* 2011, **45**, 7718-7726.
- 25 G. Sheng, H. Dong, R. Shen and Y. Li, *Chem. Eng. J.* 2013, **217**, 486-494.
- 26 G. Sheng, R. Shen, H. Dong and Y. Li, *Environ. Sci. Pollut. Res.* 2013, **20**, 3708-3717.
- 27 Y.-C. Lee, W.-K. Park and J.-W. Yang, *J. Hazard. Mater.* 2011, **190**, 652-658.
- 28 Y.-C. Lee, J.-Y. Kim and H.-J. Shin, *Sep. Sci. Technol.* 2013, **48**, 1093-1101.
- 29 S. Y. Park, H. U. Lee, Y.-C. Lee, S. Choi, D. H. Cho, H.S. Kim, S. Bang, S. Seo, S. C. Lee, J. Won, B.-C. Son, M. Yang and J. Lee, *Sci. Rep.* 2015, **4**, 12420 (1-8).
- 30 S. H. Choi, S.-H. Seok and J. S. Lee, *J. Synchrotron Rad.* 2001, **8**, 596-598.
- 31 H. P. Boehm, *Carbon* 1994, **32**, 759-769.
- 32 P. Chaturbedy, D. Jagadeesan and M. Eswaramoorthy, *ACS Nano* 2010, **4**, 5921-5929.
- 33 W. Farooq, Y.-C. Lee, J.-I. Han, C. H. Darpito, M. Choi and J.-W. Yang, *Green Chem.* 2013, **15**, 749-755.
- 34 S. L. Burkett, A. Press and S. Mann, *Chem. Mater.* 1997, **9**, 1071-1073.
- 35 A. J. Patil, M. Li, E. Dujardin and S. Mann, *Nano Lett.* 2007, **7**, 2660-2665.
- 36 Y.-C. Lee, E. J. Kim, D. A. Ko and J.-W. Yang, *J. Hazard. Mater.* 2011, **196**, 101-108.
- 37 J. Zhu, L. Wang, T. Zhou, Y. Cho, T. Suehiro, T. Takeda, M. Lu, T. Sekiguchi, N. Hirotsaki and R.-J. Xie, *J. Mater. Chem. C* 2015, **3**, 3181-3188.
- 38 C. K. Narula, W. H. Weber, J. Y. Ying and L. F. Allard, *J. Mater. Chem.* 1997, **7**, 1821-1829.
- 39 M. I. Dar, S. Sampath and S. A. Shivashankar, *RSC Adv.* 2014, **4**, 49360-49366.
- 40 G. Sheng, Q. Yang, F. Peng, H. Li, X. Gao and Y. Huang, *Chem. Eng. J.* 2014, **245**, 10-16.
- 41 G. Sheng, L. Ye, Y. Li, H. Dong, H. Li, X. Gao and Y. Huang, *Chem. Eng. J.* 2014, **248**, 71-78.

75
TOC

The recoveries of Sr^{2+} and La^{3+} as rare earth metals (REMs) were studied using Mg-aminoclay-humic acid [MgAC-HA] complexes prepared by self-assembled precipitation, i.e., [HA] intercalation into layered [MgAC], due to electrostatic attraction between water-solubilized [MgAC] and water-soluble [HA].

